Supporting Information for

Rational design of N-doped CNTs@C_3N_4 network for dual-capture of biocatalysts in enzymatic glucose/O_2 biofuel cells

Gangyong Li, [a,b] Guangming Ren, [c] Wei (Alex) Wang, [d] and Zongqian Hu [b*]

[a]*State Key Laboratory of Advanced Metallurgy, University of Science and Technology Beijing, Beijing, 100083, P. R. China*

[b]*Beijing Institute of Radiation Medicine, Beijing, 100850, P. R. China. E-mail: huzongqian@hotmail.com*

[c] *Beijing Institute of Lifeomics, Beijing, 102206, P. R. China*

[d]*Beijing Key Laboratory of Bio-inspired Energy Materials and Devices, School of Space and Environment, Beihang University, Beijing, 100191, P. R. China*

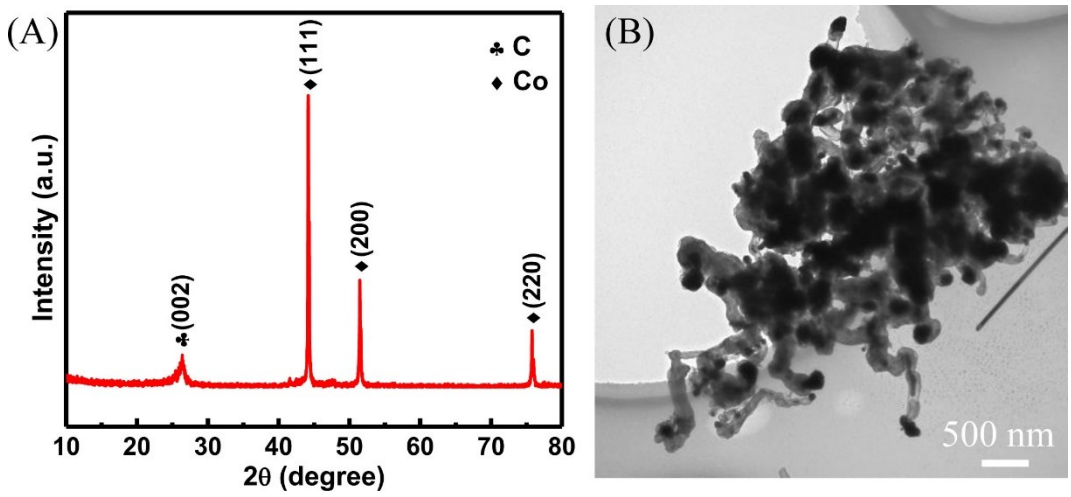

Fig. S1 (A) XRD pattern and (B) TEM image of Co@N-CNTs@C_3N_4.

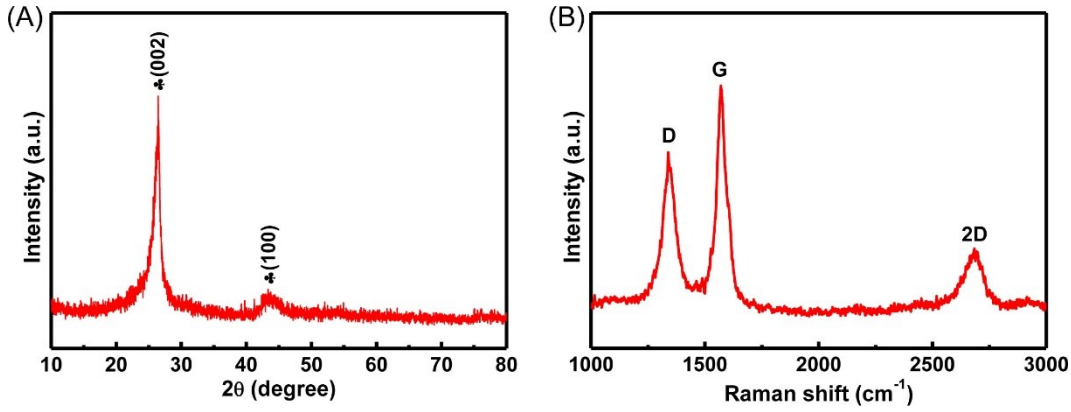

Fig. S2 (A) XRD pattern and (B) Raman spectrum of N-CNTs@C_3N_4 after washing with HCl.

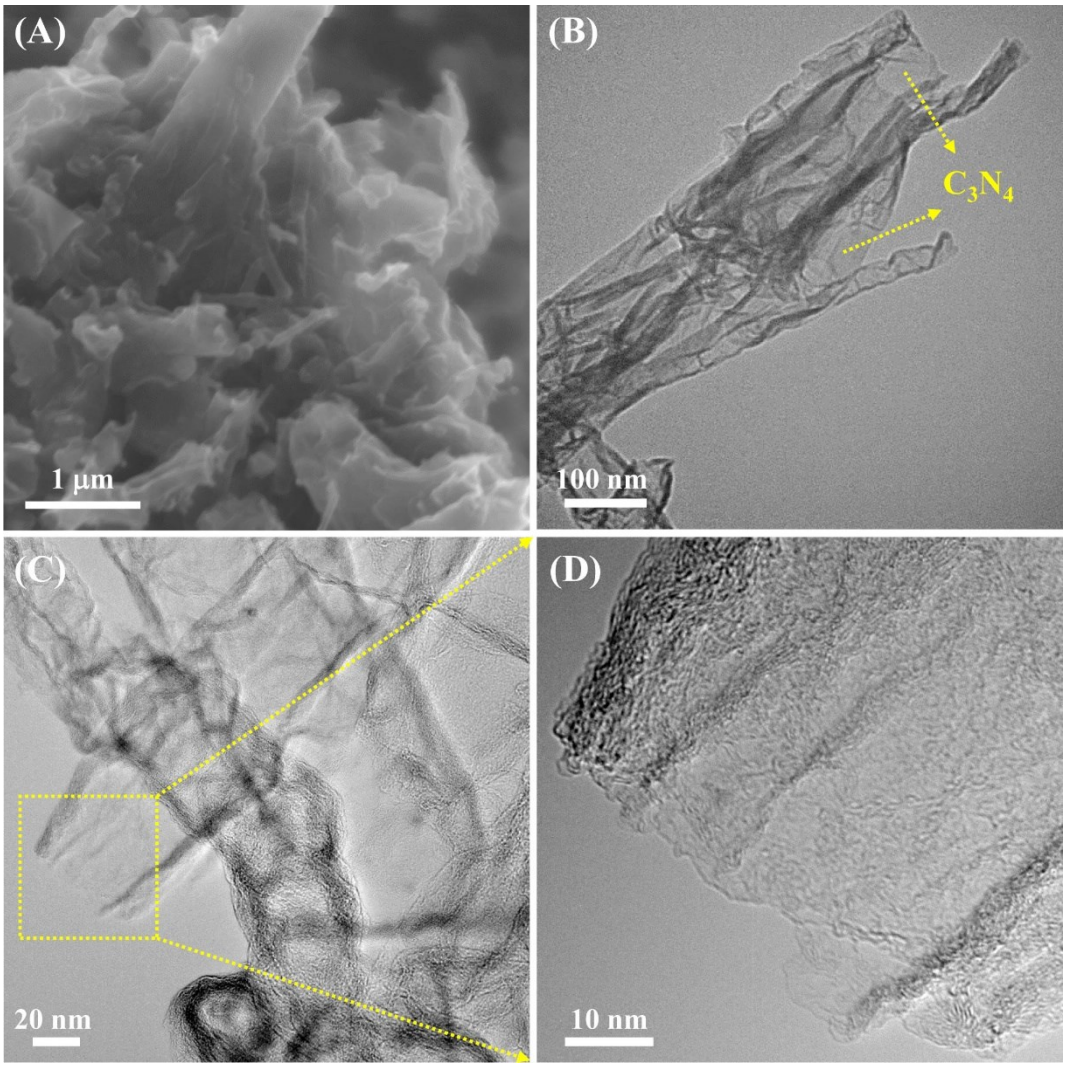

Fig. S3 (A) SEM and (B-D) TEM images of N-CNTs@C_3N_4.

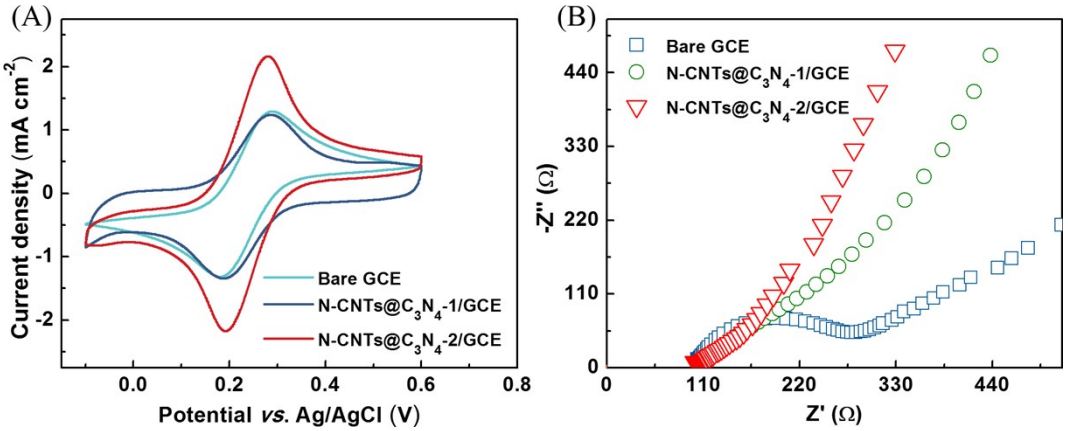

Fig. S4 (A) CV curves and (B) Nyquist plots of bare GCE, N-CNTs@C_3N_4-1/GCE, and N-CNTs@C_3N_4-2/GCE with 5 mM $[Fe(CN)_6]^{3-/4-}$ in 0.1 M KCl solution. Scan rate = 50 mV s^{-1}.

The electrochemical performance of bare GCE, N-CNTs@C_3N_4-1 (after washing with HCl), and N-CNTs@C_3N_4-2 (after washing with HCl and then thermal annealing at 1600 °C for 2 h) modified GCE was investigated using CV and EIS. **Fig. S4A** provides CV curves of bare GCE, N-CNTs@C_3N_4-1/GCE, and N-CNTs@C_3N_4-2/GCE with 5 mM $[Fe(CN)_6]^{3-/4-}$ in 0.1 M KCl solution at 50 mV s^{-1}. The three electrodes exhibit a well-defined redox peak. Note that N-CNTs@C_3N_4-2/GCE manifests higher faradaic current and lower peak-to-peak separation (ΔE_p) value than those of bare GCE and N-CNTs@C_3N_4-2/GCE, indicating high electroactive area and fast electron transfer kinetics of N-CNTs@C_3N_4-2/GCE. **Fig. S4B** depicts EIS results of the three electrodes. The diameter of the semicircles in the high- and middle-frequency represents the charge transfer resistance. No obvious semicircles can be found in N-CNTs@C_3N_4-1/GCE and N-CNTs@C_3N_4-2/GCE, indicating faster electron transfer kinetics within the N-CNTs@C_3N_4 modified electrode than bare GCE. Therefore, it is expected that the immobilization of enzymes on N-CNTs@C_3N_4 modified electrode would improve the electrochemical performance due to its enhanced electrical conductivity.

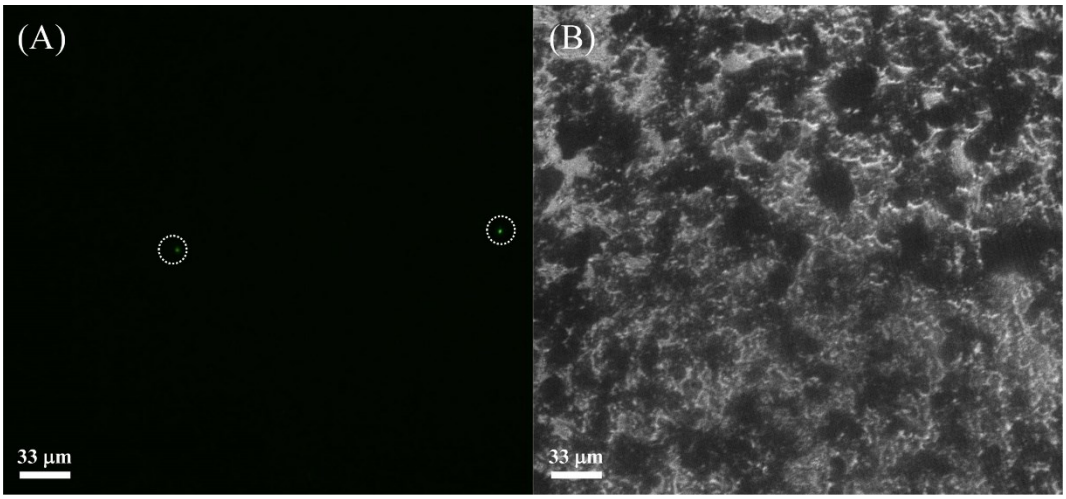

Fig. S5 CLSFM images of N-CNTs@C_3N_4 in the absence of GOx under excitation light (A) and under objective (B). The white dotted circles in **Fig. S5A** mark out the sparse fluorescent spots.

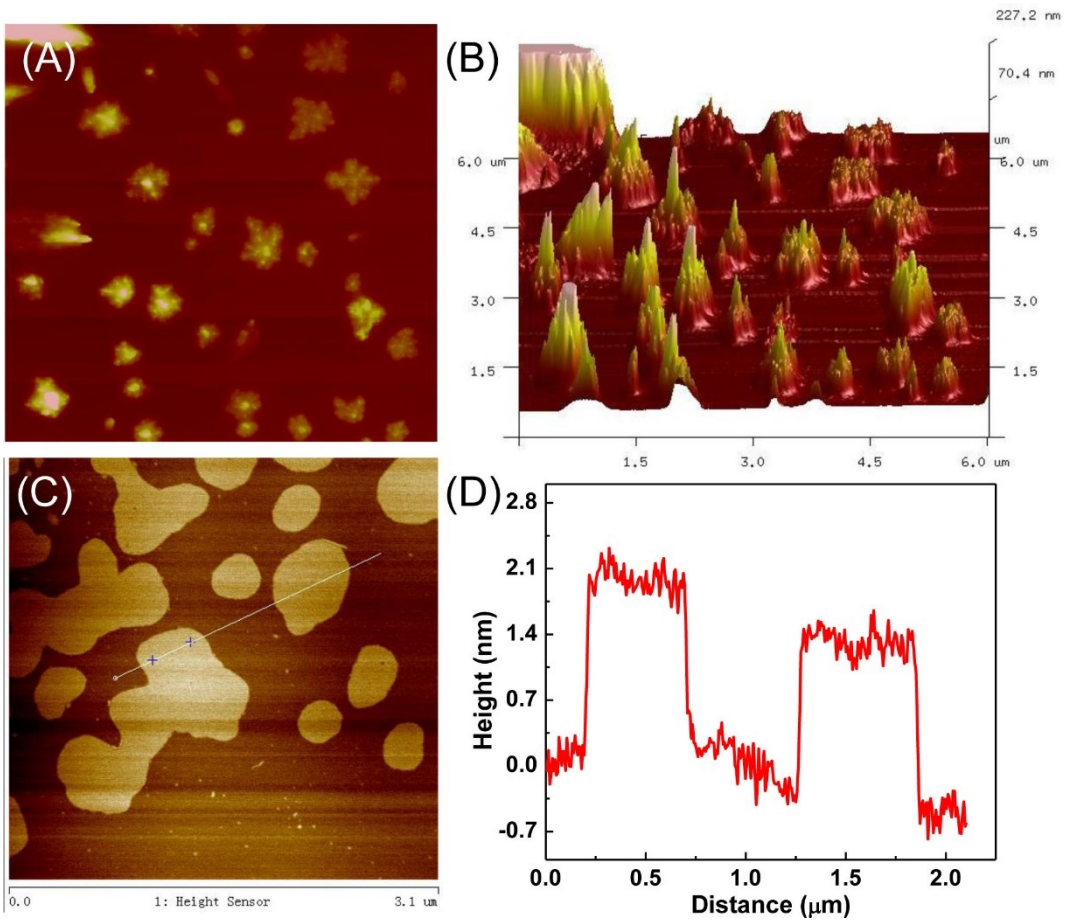

Fig. S6 (A) 2D and (B) 3D AFM images of N-CNTs@C_3N_4. (C) 2D AFM image of C_3N_4 nanosheets. (D) Height profile of the trace line in **Fig. S6C**.

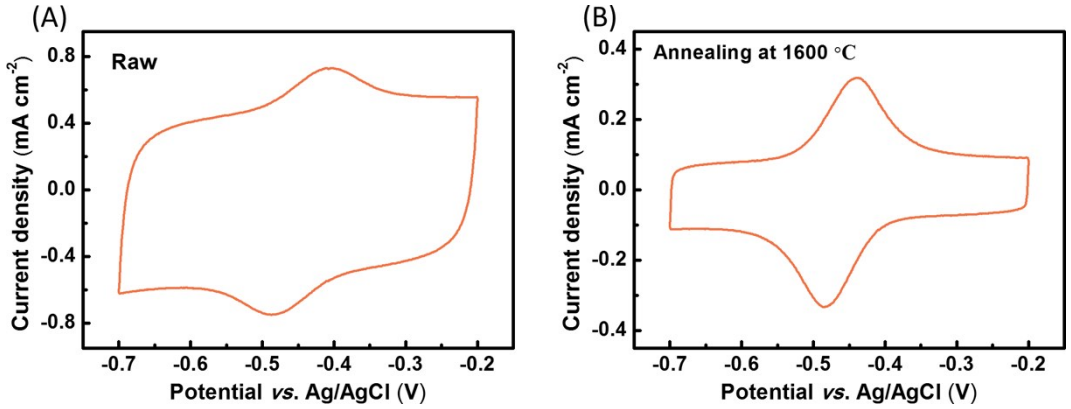

Fig. S7 CV curves of GOx/N-CNTs@C_3N_4/GCE in 0.1 M PBS (pH 7.2) saturated with Ar. Scan rate: 50 mV s^{-1}. (A) N-CNTs@C_3N_4 after washing with HCl. (B) N-CNTs@C_3N_4 after washing with HCl and then thermal annealing at 1600 °C for 2 h.

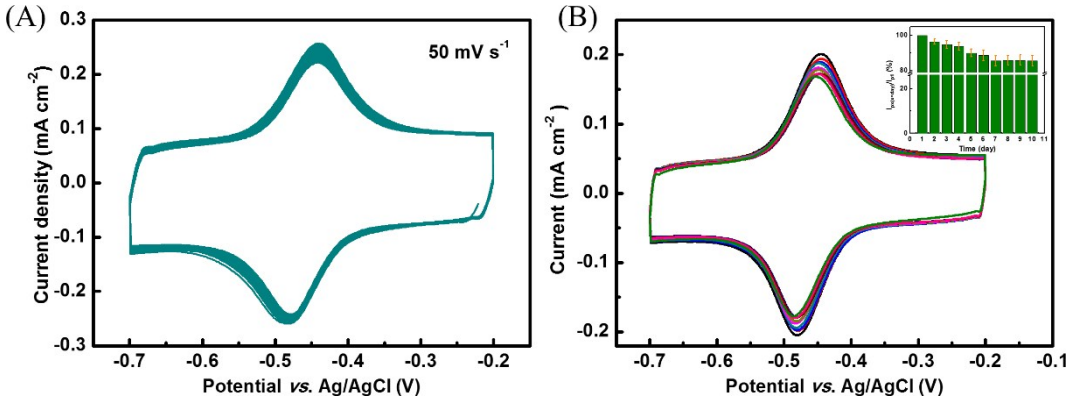

Fig. S8 (A) CV curves of GOx/N-CNTs@C_3N_4/GCE in Ar-saturated 0.1 M PBS (pH 7.2) at 50 mV s^{-1} for 200 cycles. (B) CV curves of GOx/N-CNTs@C_3N_4/GCE in Ar-saturated 0.1M PBS (pH 7.2) for 10 days by once a day. Scan rate = 50 mV s^{-1}. Inset shows the I_P/I_{P1} (%) of 3 electrodes.

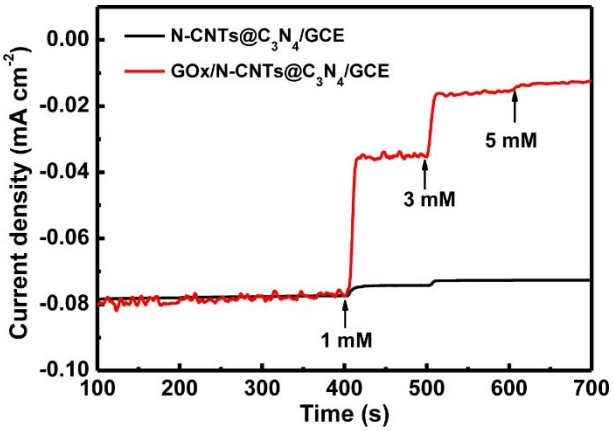

Fig. S9 Comparison of amperometric response of the GOx/N-CNTs@C_3N_4/GCE and N-CNTs@C_3N_4/GCE to successive addition of glucose in 0.1 M PBS (pH 7.2) at an applied potential of -0.42 V.

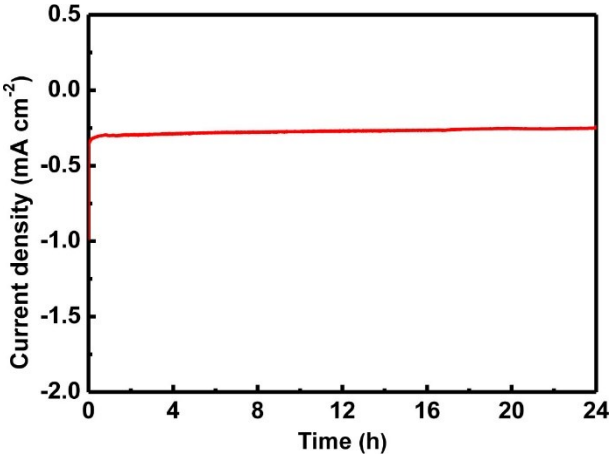

Fig. S10 Chronoamperometry (i-t) curve of Lac/N-CNTs@C_3N_4/GCE biocathode collected at 0 V (*vs*. Ag/AgCl) in O_2-saturated 0.04 M B-R solution (pH 5.0).

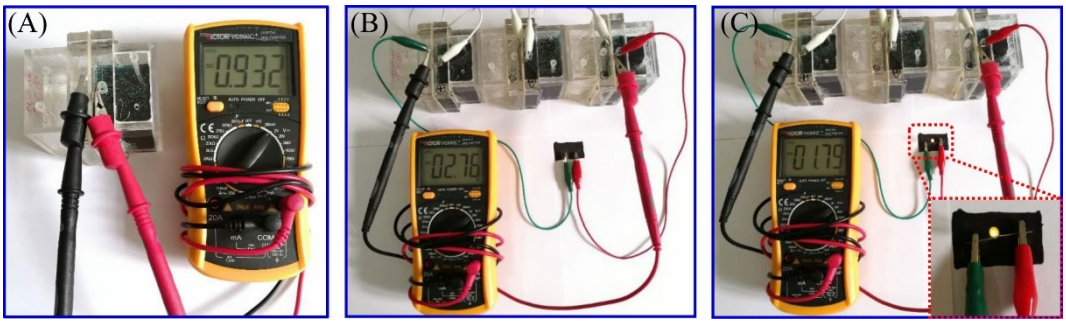

Fig. S11 (A) Digital photograph of a single glucose/O_2 BFC showing a high OCP of 0.932 V. (B) Digital photograph of three glucose/O_2 BFCs in series generating an OCP of 2.76 V. (C) Digital photograph of three glucose/O_2 BFCs in series powering a yellow LED lamp.

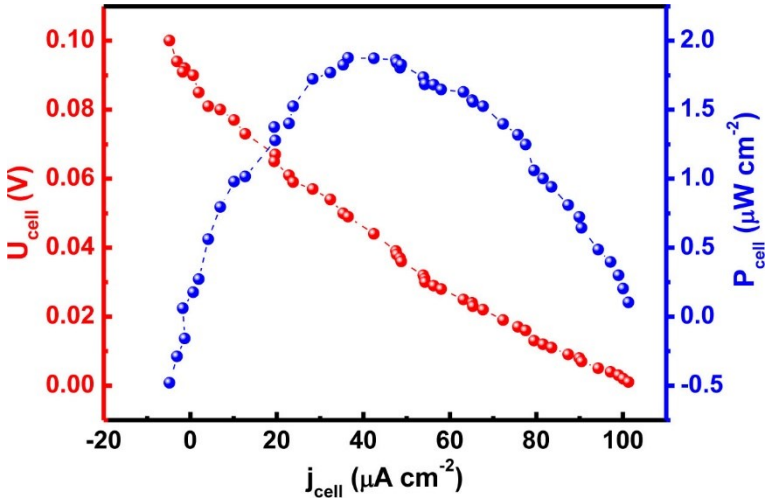

Fig. S12 Dependence of the U_{cell} and P_{cell} on the j_{cell} for the fuel cell in the absence of enzymes under ambient air.

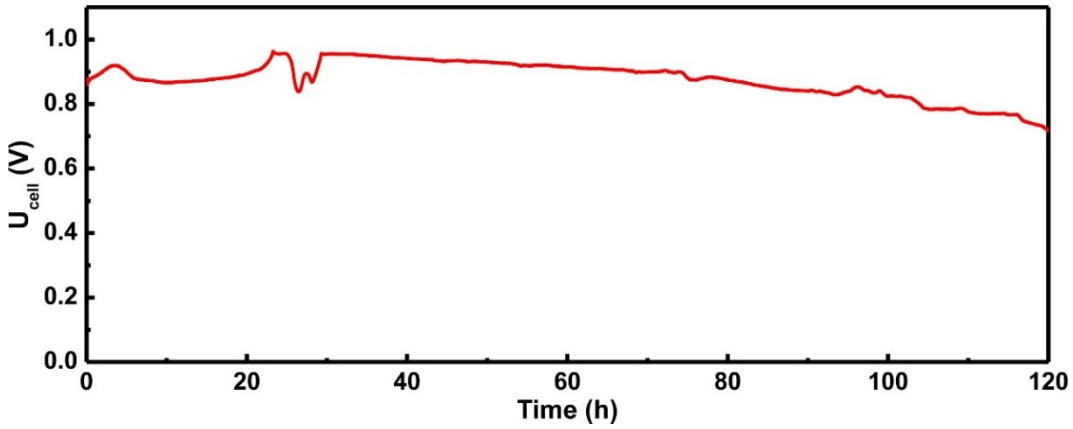

Fig. S13 U_{cell} *vs*. time for the fabricated glucose/O_2 BFC continuously operating at 100 kΩ for 120 h.

Table S1 Comparison of electrochemical parameters of the GOx modified electrodes[a].

Modified electrode	E'^0 (mV)	pH	k_s (s^{-1})	Γ^* (mol cm^{-2})	Ref.
GOx/N-CNTs@C_3N_4/GCE	-457	7.2	4.78	8.26×10^{-10}	This work
AuNPs/GOD-CNT-PVA/GC	-504	7.0	2.2	2.56×10^{-10}	1
GCNT/GOD/GAD/GC	-400	7.0	1.08	3.88×10^{-9}	2
GOD/NH_2–TiO_2–CNT/GC	-460	7.4	3.5	8.77×10^{-11}	3
GOD/PDDA-HCNTs/MGC	-476.5	7.4	–	1.36×10^{-10}	4
NF/ZnO/$(PSS/PDDA)_3$/GOD/ITO/GC	-105	6.0	2.16	3.57×10^{-11}	5
NF/GOD-MC/GC	-437.5	7.0	4.1	3.62×10^{-12}	6

[a] GOx = glucose oxidase; N-CNTs = N-doped carbon nanotubes; C_3N_4 = carbon nitride; GCE = glassy carbon electrode; AuNPs = gold nanoparticles; GOD = glucose oxidase; PVA = polyvinyl alcohol; GC = glassy carbon; GCNT = gelatin-multiwalled carbon nanotube; GAD = glutaraldehyde; PDDA-HCNTs = poly(diallyldimethylammonium chloride) functionalized helical carbon nanotubes; MGCE = magnetic glass carbon electrode; PSS = poly(sodium 4-styrensulfonate); ITO = indium tin oxide; MC= mesoporous carbon FDU-15.

References

1 H. Zhang, Z. Meng and Q. Wang, J. Zheng, *Sens Actuators B*, 2011, **158**, 23-27.

2 A. P. Periasamy, Y. J. Chang and S. M. Chen, *Bioelectrochemistry*, 2011, **80**, 114-120.

3 M. Tasviri, H. A. Rafiee-Pour, H. Ghourchian and M. R. Gholami, *J. Mol. Catal. B, Enzym*., 2011, **68**, 206-210.

4 R. Cui, Z. Han, J. Pan, E. S. Abdel-Halim and J. J. Zhu, *Electrochim. Acta*, 2011, **58**, 179-183.

5 Y. Zhai, S. Zhai, G. Chen, K. Zhang, Q. Yue, L. Wang, J. Liu and J. Jia, *J. Electroanal. Chem*., 2011, **656**, 198-205.

[6] K. Wang, H. Yang, L. Zhu, Z. Ma, S. Xing, Q. Lv, J. Liao, C. Liu and W. Xing, *Electrochim.*

Acta, 2009, **54**, 4626-4630.

Table S2 Performance of 3D structures as bioelectrodes applied in EBFC application[b].

Anode	Cathode	OCP (V)	P_{max} (mW cm^{-2})	Ref.
GOx/N-CNTs@C_3N_4/Ni foam	**Lac/N-CNTs@C_3N_4/Ni foam**	**0.93**	**0.570**	**This work**
GOx/OMCs/GCE	Pt	1.20	0.110	1
GOx/3D-GNs/Fc/GCE	Lac/3D-GNs-PTCA-DA/GCE	0.38	0.112	2
GOx/C-MEMS	Lac/C-MEMS	0.91	0.136	3
GOx/GN/SWCNTs aerogel	BOD/GN/SWCNTs aerogel	0.61	0.190	4
GOx/CP/LPEI-C_6/Fc	Lac/CP/MWCNTs/TBAB	0.55	0.024	5
GOx/Pd aerogel/β-cyclodextrin/Fc	BOD/Pd-Pt aerogel	0.40	0.020	6
GOx/$PANI_{1600}$@GO/GCE	Pt-C/GCE	0.76	0.756	7
GOx/$PANI_{1600}$@GO/CP	Lac/$PANI_{1600}$@GO/CP	0.78	1.120	8
GOx/PCP/GCE	Pt-C/GCE	0.68	0.548	9
GOx/CNCs/GCE	Pt	0.59	0.055	10
GOx/PAE	BOD/PAE	0.77	0.132	11
GOx/Carbonized RPPy	Lac/Carbonized RPPy	1.16	0.350	12
GOx/NQ-LPEI	BOD/AnMWCNT	0.78	0.36	13
GOx/TTF/BP	Lac/BP	0.511	0.018	14
GOx/AuNPs/CP	Lac/SWCNTs/CP	0.60	0.053	15
GOx/CoPc/PBA/BP	MnO_2/PBA/BP	0.65	0.136	16

[b] GOx = glucose oxidase; N-CNTs = N-doped carbon nanotubes; C_3N_4 = carbon nitride; Lac = laccase; OMCs = ordered mesoporous carbon; GCE = glassy carbon electrode; 3D-GNs = three-dimensional graphene networks; Fc = ferrocence; PTCA = 3,4,9,10-perylene tetracarboxylic acid; DA = dopamine; C-MEMS = carbon microelectromechanical systems; GN = graphene; SWCNTs = single-wall carbon nanotubes; BOD = bilirubin oxidase; CP = carbon paper; LPEI = linear polyethyleneimine; TBAB = tetrabutylammonium bromide; GDH = glucose dehydrogenase; PANI = polyaniline; GO = graphene oxide; PCP = porous

coordination polymers; CNCs = carbon nanochips; PAE = Au nanoparticle-modified paper fibers; RPPy = rectangular polypyrrole; NQ-LPEI = naphthoquinone-LPEI; AnMWCNT = anthracene-modified MWCNT; TTF = tetrathiafulvalene; BP = buckypaper; CoPc = cobalt phthalocyanine; PBA = 1-pyrenebutyric acid.

References

1 C. X. Guo, F. P. Hu, X. W. Lou and C. M. Li, *J. Power Sources*, 2010, **195**, 4090-4097.

2 Y. Zhang, M. Chu, L. Yang, Y. Tan, W. Deng, M. Ma, X. Su and Q. Xie, *ACS Appl Mater Interfaces*, 2014, **6**, 12808-12814.

3 Y. Song, C. Chen and C. Wang, *Nanoscale*, 2015, **7**, 7084-7090.

4 A. S. Campbell, Y. J. Jeong, S. M. Geier, R. R. Koepsel, A. J. Russell and M. F. Islam, *ACS Appl. Mater. Interfaces*, 2015, **7**, 4056-4065.

5 M. Jose Gonzalez-Guerrero, F. Javier del Campo, J. Pablo Esquivel, F. Giroud, S.D. Minteer and N. Sabate, *J. Power Sources*, 2016, **326**, 410-416.

6 D. Wen, W. Liu, A. K. Herrmann and A. Eychmueller, *Chem. Eur. J.*, 2014, **20**, 4380-4385.

7 Z. Kang, K. Jiao, X. Xu, R. Peng, S. Jiao and Z. Hu, *Biosens. Bioelectron.*, 2017, **96**, 367-372.

8 Z. Kang, K. Jiao, J. Cheng, R. Peng, S. Jiao and Z. Hu, *Biosens. Bioelectron.*, 2018, **101**, 60-65.

9 Z. Kang, K. Jiao, R. Peng, Z. Hu and S. Jiao, *RSC Adv.*, 2017, **7**, 11872-11879.

10 Z. Kang, K. Jiao, C. Yu, J. Dong, R. Peng, Z. Hu and S. Jiao, *RSC Adv.*, 2017, **7**, 4572-4579.

11 Y. Wang, L. Zhang, K. Cui, S. Ge, P. Zhao and J. Yu, *ACS Appl. Mater. Interfaces*, 2019, **11**, 5114-5122.

12 Z. Kang, Y.-H. P. J. Zhang and Z. Zhu, *Biosens. Bioelectron.*, 2019, **132**, 76-83.

13 R. A. Escalona-Villalpando, K. Hasan, R. D. Milton, A. Moreno-Zuria, L. G. Arriaga, S. D. Minteer and J. Ledesma-García, *J. Power Sources*, 2019, **414**, 150-157.

14 P. Rewatkar, Jayapiriya U. S and S. Goel, *ACS Sustainable Chem. Eng.*, 2020, **8**, 12313-

12320.

15 J. Wan, L. Mi, Z. Tian, Q. Li and S. Liu, *J. Mater. Chem. B*, 2020, **8**, 3550-3556.

16 S. Hao, H. Zhang, X. Sun, J. Zhai and S. Dong, *Nano Res*., 2021, **14**, 707-714.

Table S3. The performances of the glucose/O_2 BFCs directly using four different kinds of soft drinks: iced red tea, aerated water, orange juice, and coconut juice. Price here means the price of 1 mL of soft drinks utilized in the glucose/O_2 BFCs.

Soft drinks	U_{cell} (V)	P_{cell} (mW cm^{-2})	Price ($)
Iced red tea	0.815	0.414	0.00066
Aerated water	0.864	0.344	0.00043
Orange juice	0.796	0.349	0.0011
Coconut juice	0.708	0.045	0.0024

Equations

$$E_{pc} = E^{'0} - \left[\frac{RT}{\alpha nF}\right] In\left[\frac{\alpha Fn}{RTk_s}v\right] \quad \text{(S1)}$$

$$E_{pa} = E^{'0} + \left[\frac{RT}{(1-\alpha)nF}\right] In\left[\frac{(1-\alpha)Fn}{RTk_s}v\right] \quad \text{(S2)}$$

where $E^{'0}$ is the formal potential, α is the charge transfer coefficient of the system, v is the scan rate, n is the electron transfer number in the reaction, k_s is the heterogeneous electron transfer rate constant, T, R, and F are temperature, the ideal gas constant and Faraday's constant, respectively.

$$Logk_s = \alpha Log(1-\alpha) + (1-\alpha)Log\alpha - Log\left(\frac{RT}{nFv}\right) - \alpha(1-\alpha)\left(\frac{nF\Delta E_p}{2.3RT}\right) \quad \text{(S3)}$$

$$i_{pc} = \frac{n^2F^2A\Gamma^*}{4RT}v \quad \text{(S4)}$$

Where i_{pc} is the cathodic peak current, v is the scan rate, n is the number of electron transfer, Γ^* is the surface coverage of enzyme, T, R, and F are temperature, the ideal gas constant and Faraday's constant, respectively.